

Electronic surface states in semiconductor superlattices: The case of a triple-constituent superlattice

P. Masri and M. D. Rahmani

*Laboratoire d'Etudes des Surfaces, Interfaces et Composants, Université des Sciences et Techniques du Languedoc,
place Eugène Bataillon, 34060 Montpellier CEDEX, France*

(Received 19 October 1988; revised manuscript received 21 February 1989)

For the first time a calculation is made for the dispersion relations of electronic surface states of triple-constituent semiconductor superlattices, within the framework of an analytical model of interaction. An application is presented for a GaSb/AlSb/InAs polytype superlattice. We show that a new electronic surface transition occurs which is associated with In-derived surface states.

I. INTRODUCTION

The properties of semiconductor superlattices have been widely investigated, and studies have mainly considered dual-constituent systems.¹ Superlattice growth techniques, such as molecular-beam epitaxy (MBE) or metallo-organic chemical vapor deposition (MOCVD), have until now concerned these systems. As a consequence of the synthesis of a wide variety of man-made superlattices, device physics was afforded numerous potential electronic applications. This has led to much basic research in heterostructure systems. One straightforward issue for such applications concerns the fabrication of lattice-matched material systems characterized by a band-gap and a refractive-index variable. An example of this is the two-constituent GaAs/Al_xGa_{1-x}As hot-electron transistor² (HET). Unfortunately, as the injected hot electrons present a high scattering rate for collisions with impurities in the heavily doped transistor base,³ it was concluded that GaAs was not the best choice for high-performance HET.

Another heterostructure, GaSb/InAs, has been proposed as an alternative.⁴ This system belongs to the so-called type-2 misaligned superlattice family and provides very interesting features of the discontinuities of band-edge energies in which the bottom of the conduction band in InAs is located below the top of the valence band in GaSb. The consequence of such an interpenetration between the valence and conduction constituent bands is the creation of a nonrectifying *p-n* junction from which the superlattice is built up. This produces an electron flow from the GaSb valence band to the InAs conduction band and thus the creation of a dipole layer associated with the two-dimensional induced electrons and holes. The introduction of a potential barrier (AlSb) in such a system may offer new possibilities for device applications.⁵ In such systems, the band-discontinuity mechanism leads to an "intrinsic" creation of free carriers (electrons in InAs layers and holes in GaSb layers) and the major disadvantage (collisions with impurities) due to extrinsic doping is avoided. This feature added to those of relative band positions (the large AlSb/InAs conduction-band discontinuity and large barrier height provided by AlSb layers) makes the GaSb/AlSb/InAs polytype super-

lattice a very attractive one. However, one must be aware of the difficulties encountered in growing such systems. This materials-science aspect has been discussed recently.³ The difficulties may arise because of the lattice mismatch between the different materials. Depending on the experimental growth conditions, significant interfacial dislocation density may be produced. Nevertheless, technological interest in such devices stimulates basic research to understand their solid-state features.

In a recent study, we calculated the bulk dispersion relations for electrons in a polytype GaSb/AlSb/InAs superlattice. This was done by applying a recently proposed interface response theory^{6,7} to study electronic bulk excitations in *N*-layer discrete semiconductor superlattices. The different possible surfaces of such a system may present specific features which are investigated in this work by extending the theory to the surface case. The dispersion relations of electronic surface states are calculated, and their dependence on layer thickness is then discussed. It should be pointed out that the electronic surface states in dual-constituent semiconductor superlattices have been previously studied by using a Green's-function method within the framework of a simple two-band model.⁸

II. GENERAL FORMALISM AND MODEL

A. Model

The main features of the two-band model used in this work should first be brought to mind. It is possible to reasonably describe the lowest conduction band near the Brillouin-zone center and the valence bands for homogeneous and heterogeneous semiconductors. This is done by using a tight-binding Hamiltonian restricted by nearest-neighbor interactions and represented in a minimal basis consisting of one *s*- and three *p*-electron states, namely *sp*³ orbitals localized on each lattice site.⁹ While the lowest conduction band is nondegenerate and has a minimum energy at the zone center, the upper valence band is doubly degenerate, consisting of heavy- and light-hole branches with a degeneracy occurring at the center of the Brillouin zone. Spin-orbit splitting drops one of the heavy-hole bands to lower energies. If

one is interested in electron states falling in the neighborhood of the gap, it is possible to make further approximations by disregarding the s orbitals on the nonmetallic atoms in the compound and the p orbitals on the metallic atoms. This is true because their associated energies are situated outside the relevant energy domain, contributing slightly to the corresponding electron states.

The interaction parameters relevant to this model¹⁰ include (i) two orbital self-energies, E_1 and E_2 , associated, respectively, with atoms of type 1 and 2 constituting each material, and (ii) the hopping integrals γ_i characterizing the nearest-neighbor interactions. The Hamiltonian \underline{H}_{0i} associated with this model has the following expression:

$$H_{0i}(|\beta; l'\beta'\rangle) = \langle l\beta | \underline{H}_{0i} | l'\beta'\rangle \quad (1a)$$

with nonzero elements

$$\langle l\beta | \underline{H}_{0i} | l\beta\rangle = E_\beta, \quad \beta=1,2 \quad (1b)$$

and nearest-neighbor off-diagonal elements (hopping integrals)

$$\langle l1 | \underline{H}_{0i} | l2\rangle = \gamma_{li} = \gamma_i \quad (1c)$$

with

$$\langle l\beta | l'\beta'\rangle = \delta_{ll'}\delta_{\beta\beta'}, \quad (1d)$$

where $(l\beta)$ represents the position of the β th-type basis atom in the l th unit cell of the crystal; $\beta=1$ or 2 for the two types of atoms in the unit cell.

The bulk electronic states of material of type (i) are then obtained in the form of the energy spectrum of the bulk response function \underline{G}_{0i} given by the following relationship:

$$\underline{H}_{0i}\underline{G}_{0i} = \underline{I}, \quad (2)$$

where \underline{I} is the unit matrix. The following dispersion relations are then obtained:

$$E_i = (E_{1i} + E_{2i})/2 \pm \left[\frac{(E_{1i} - E_{2i})/2)^2 + 64\gamma_i \prod_{j=1}^3 \cos^2(k_j a_0/2)}{2} \right]^{1/2}, \quad (3)$$

where $k = (k_1, k_2, k_3)$ is the wave vector. For our (001)-surface problem, we can use the wave-vector representation $[k_\parallel(k_1, k_2)]$ parallel to the (001) plane (Fourier transformation). The analytic expressions of the elements of \underline{G}_{0i} referring to type-1 and -2 atoms are¹⁰

$$G_{0i}(\mathbf{k}_\parallel, l_3 1; l'_3 1; E) = a_i t_i^{|l_3 - l'_3| + 1} / [f_i^2(t_i^2 - 1)], \quad (4a)$$

$$G_{0i}(\mathbf{k}_\parallel, l_3 2; l'_3 2; E) = -d_i t_i^{|l_3 - l'_3| + 1} / [f_i^2(t_i^2 - 1)], \quad (4b)$$

$$G_{0i}(\mathbf{k}_\parallel, l_3 1; l'_3 2; E) = -\chi^*(t_i^{|l_3 - l'_3|} + t_i^{|l_3 - l'_3| - 1}) / [f_i(t_i^2 - 1)], \quad (4c)$$

$$G_{0i}(\mathbf{k}_\parallel, l_3 2; l'_3 1; E) = -\chi(t_i^{|l_3 - l'_3|} + t_i^{|l_3 - l'_3| + 1}) / [f_i(t_i^2 - 1)], \quad (4d)$$

where

$$a_i = E - E_{2i}, \quad (5a)$$

$$d_i = E - E_{1i}, \quad (5b)$$

$$\chi = e^{ia_0(k_1 + k_2)/2}, \quad (5c)$$

$$f_i = 4\gamma_i \cos(k_1 a_0/2) \cos(k_2 a_0/2), \quad (5d)$$

$$t_i = \begin{cases} \xi_i - (\xi_i^2 - 1)^{1/2}, & \xi_i > 1 \\ \xi_i + i(1 - \xi_i^2)^{1/2}, & -1 < \xi_i < 1 \\ \xi_i + (\xi_i^2 - 1)^{1/2}, & \xi_i < -1 \end{cases}, \quad (6)$$

with

$$\xi_i(\mathbf{k}_\parallel, E) = -1 + a_i d_i / 2f_i^2. \quad (7)$$

B. Interface response operator

Let us now describe the general scheme in building up an N -layer infinite or semi-infinite superlattice, as well as the corresponding relevant quantities required by the superlattice interface response theory. This allows us to obtain all information about their bulk and electronic surface states. Each material [of type (i)] constituting the superlattice is formed out of L equivalent "principal layers" defined by a layer index l , with $1 \leq l \leq L_i$. This is obtained by truncating an infinite crystal on both sides to produce a finite-size slab. This procedure, involving the cancellation of interactions between this slab and the remaining part of the crystal, is represented by the "cleavage" operator \underline{V}_s . The next step is to couple these different slabs together to build up the superlattice. To achieve this coupling, we introduce interfacial interactions between the different slabs forming the N -layer superlattice. These interactions are represented by the interface coupling operator \underline{V}_l which binds the free-surface slabs together. The complete interface response operator \underline{A}' is then defined by the following relationship:

$$\underline{A}' = \underline{A}'_s + \underline{V}_l \underline{G}, \quad (8)$$

where \underline{G} is the bulk response function, giving all electronic bulk properties of the new superlattice material. This quantity \underline{G} is indeed the reference quantity in the theory. The final energy spectrum associated with the heterostructure originates from the modified spectrum of \underline{G} . The modifications arise from the creation of the superlattice as a new periodicity appears (band folding) and new interactions are introduced (interactions between separate material bands leading to the final band structure). In Eq. (8), \underline{A}'_s is the surface response operator of the N -layer superlattice.⁷

The elements of the N -layer superlattice response function \underline{g} can be calculated by using the general relationship⁶

$$(\underline{I} + \underline{A}') \cdot \underline{g} = \underline{G}. \quad (9)$$

Once this response function is known, one can calculate the electronic spectrum associated with the N -layer superlattice. In particular, for a triple-constituent superlattice the dispersion relations of bulk electronic bands

are given by the following expression:¹¹

$$2\eta(k_{\parallel}, E) = -A_1 A_2 A_3 + B_1 B_2 B_3 + |\epsilon_{ijk}| \left[\frac{\tilde{f}_j}{\tilde{f}_i} a_i d_j A_k - \frac{\tilde{f}_i}{\tilde{f}_j} a_j d_i B_k \right] C_i C_j, \quad (10)$$

where Einstein's summation rule for tensors is used and the Levi-Civita symbol is

$$\epsilon_{ijk} = \begin{cases} 1 & \text{if } i, j, k \text{ is an even permutation of } 1, 2, 3 \\ -1 & \text{if } i, j, k \text{ is an odd permutation of } 1, 2, 3 \\ 0 & \text{in other cases.} \end{cases}$$

k_3 is the component of the wave vector perpendicular to the layer plane; a_u represents the width of the superlattice unit cell defined by the relationship

$$a_u = a_0 \sum_{i=1}^N L_i, \quad (11)$$

a_0 being the constituent lattice parameter, assumed equal for all constituents. The associated superlattice subbands enable us to localize the superlattice gaps within which electronic surface states may exist.

The general expressions of the elements of g , as well as the quantities appearing in Eq. (3), have been given elsewhere.¹¹ In the following, we will concentrate on the superlattice surface problem. From this viewpoint, an N -layer superlattice may afford many surface configurations depending on the material and the atomic species by which the growth sequence ends. If, for example, we consider a three-layer system, six configurations are possible for polar surfaces, with two configurations associated with each top layer. The configuration choice may depend on the material with which this semi-infinite structure makes contact. We are dealing here with a problem similar to that of single-crystal surface physics as new superlattice electronic surface properties may arise. It is obviously important to determine these properties as a first step in the characterization of the initial state of the semi-infinite superlattice prior to its utilization as a substrate material. New questions arise concerning, for example, the relation between the surface symmetry of the boundary material in the superlattice and what we may expect for the separated semi-infinite material. The occurrence of new superlattice surface structures related, to some extent, to the processes within the more or less abrupt interfacial transition regions between the constituent materials may be seen as an important issue. As is the case for single-crystal surface studies, the transferability of the bulk parameters to the superlattice surface may be considered as a first approximation, although specific alterations of these parameters may be expected. On the other hand, by assuming a translational symmetry in the surface plane, a Fourier analysis of the electronic states may be carried out. The corresponding states may be quantified by using the wave-vector representation (k_{\parallel}) parallel to the layer plane. As is known, due to the

lattice mismatch between the constituent materials interfacial strains may exist. Beyond a critical thickness, extended defects may appear. The emergence of these defects at the superlattice surface means that small values of $|k_{\parallel}|$ represent justified good "quantum numbers," whereas the definition of the bidimensional Brillouin zone at large values of $|k_{\parallel}|$ may be more approximative. The problems of interfacial strain and extended defects are indeed relevant to superlattice technology. This is true because the aim is to produce structures with interfacial regions free of extended defects.

Bearing all these problems in mind, we will give the expressions of the physical quantities which enable us to calculate the superlattice electronic surface states in the following section.

C. The superlattice surface case

Following the general scheme outlined in Ref. 8, and using surface-physics terminology, we create two superlattice free surfaces by introducing a "cleavage" plane between two adjacent materials i and i' . This has the effect of canceling all interactions between planes ($n=0, i=N, l_3=L_N, \beta=2$) and ($n=1, i=1, l_3=1$,

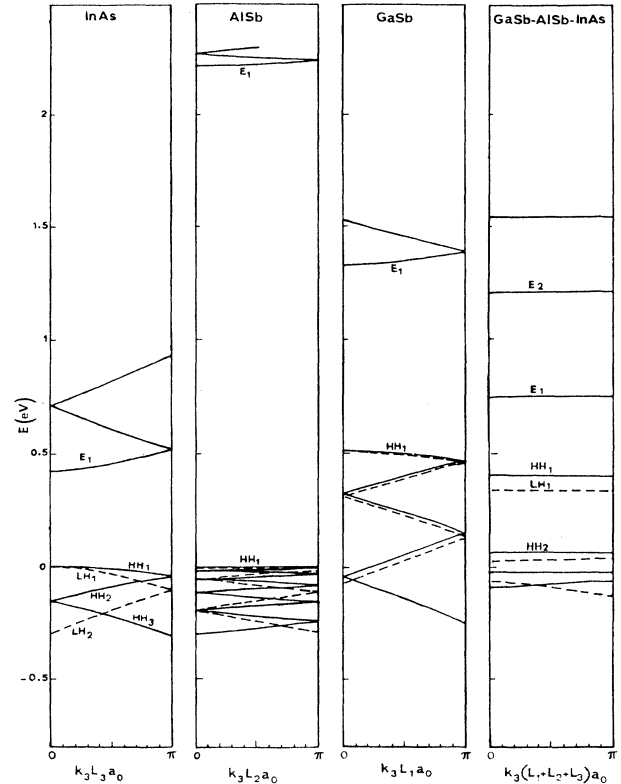


FIG. 1. Dispersion relations of the bulk bands of InAs, AlSb, GaSb, and of the superlattice GaSb/AlSb/InAs as a function of the wave-vector component (k_3) perpendicular to layer planes. Solid lines correspond to the light-hole and electron bands, while heavy-hole bands are shown as dashed lines. Layer thicknesses are equal to $L_1 = L_2 = L_3 = 12$.

$\beta=1$) in an N -layer superlattice. The first integer n refers to the multiconstituent (N) unit cell from which the superlattice is built up. The second index i refers to the layer type. Each layer i is made of $l_i=1$ to L_i equivalent principal layers, with atoms of type 1 or 2 for polar atomic planes. From a growth-experiment

viewpoint, this corresponds to a sample for which growth is started with type- N material and type-2 atoms, and stopped after the growth of L_1 principal layers of type-1 material (with a top layer made of type-1 atoms). The corresponding surface perturbation will result in the following surface-creation operator:

$$V_s(nl_3\beta; n'i'l'_3\beta') = -\tilde{f}_N(\delta_{n0}\delta_{iN}\delta_{l_3L_2}\delta_{\beta 2}\delta_{n'1}\delta_{i'1}\delta_{l'_3L_1}\delta_{\beta'1}\chi + \delta_{n1}\delta_{i1}\delta_{l_31}\delta_{\beta 1}\delta_{n'0}\delta_{i'N}\delta_{l'_3L_2}\delta_{\beta'2}\chi^*), \quad (12)$$

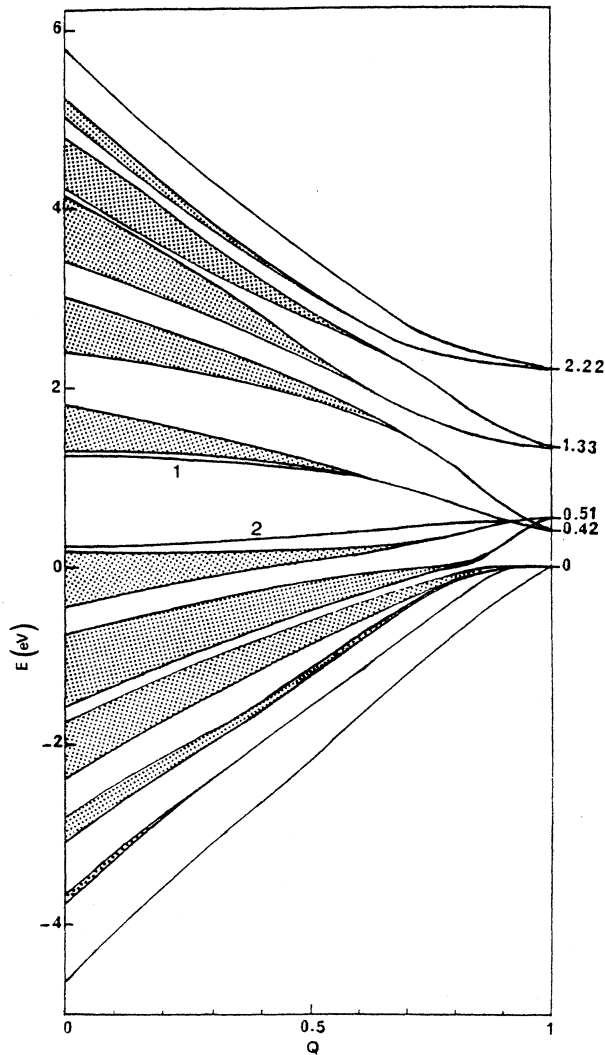


FIG. 2. Bulk and electronic surface states of a triple-constituent (GaSb/AlSb/InAs) superlattice with $L_1=L_2=L_3=2$. The bands are drawn as a function of parameter Q dependent on the wave vector parallel to the layer plane. The dashed areas correspond to the superlattice bulk bands (light-hole and electron bands). Surface states, localized within the superlattice main gap, correspond to an InAs-terminated superlattice with a cation top plane (curve 1) or an anion top plane (curve 2). The bulk bands which must converge towards the atomic levels 0.51 and 0.42 were erroneously represented in Ref. 11 in the neighborhood of $Q=1$.

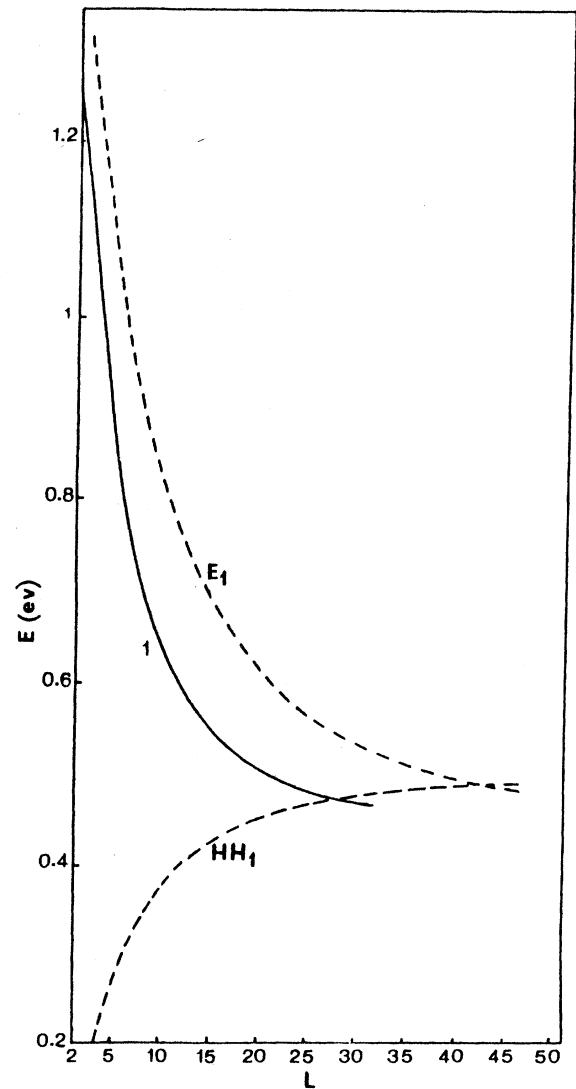


FIG. 3. Variation of the energies of the electronic surface states for an InAs-terminated GaSb/AlSb/InAs superlattice as a function of the layer thickness L . Curve 1 represents the cation (In)-derived surface state. The dashed curves show the variation of the energy of the lowest conduction subband (E_1) as well as the highest valence subband of the superlattice (HH_1) as a function of L .

where \tilde{f}_N involves the interfacial overlap integral $\tilde{\gamma}_N$ between materials N and 1,

$$\tilde{f}_N = 4\tilde{\gamma}_N \cos(k_1 a_0/2) \cos(k_2 a_0/2), \quad (13)$$

$k_{\parallel}(k_1, k_2)$ being the wave vector parallel to the interface plane. This dependence on k_{\parallel} results from the periodicity of the system in the directions along such a plane. The periodicity allows a Fourier-transformation analysis of all interaction functions resumed by the complex exponential χ .

The response function \underline{g}_s relevant to the surface problem must be calculated by using a relationship analogous to Eq. (2). In this case, a surface response operator \underline{A}'' involving both the interface response operator \underline{A}' and the effect of \underline{V}_s on the reference function $\underline{G}(\underline{G}\underline{V}_s)$ must be

used. Once the response function \underline{g}_s has been calculated, we concentrate on its denominator because it contains the key quantity D which enables us to obtain the possible surface electronic states associated with the semi-infinite superlattice. If we define

$$t_i = e^{q_i} \quad (14)$$

and¹¹

$$A_i = (\tilde{f}_i/f_i) \sinh[(L_i - \frac{1}{2})q_i] / \sinh(q_i/2), \quad (15)$$

$$B_i = (f_i/\tilde{f}_i) \sinh[(L_i + \frac{1}{2})q_i] / \sinh(q_i/2), \quad (16)$$

$$C_i = (1/f_i) \sinh(L_i q_i) / \sinh q_i, \quad (17)$$

we obtain, for a three-constituent system, the following general expressions of D :

$$D(E; i\beta; i'\beta') = -\tilde{f}_i \tilde{f}_i' C_i C_i' C_i'' (E - E_{\beta_i})(E - E_{\beta_i'})(E - E_{\beta_i''}) / \tilde{f}_i'' \\ - \tilde{f}_i'' A_i' B_i C_i'' (E - E_{\beta_i''}) + \tilde{f}_i' B_i B_i' C_i' (E - E_{\beta_i'}) + \tilde{f}_i A_i' A_i'' C_i (E - E_{\beta_i}). \quad (18)$$

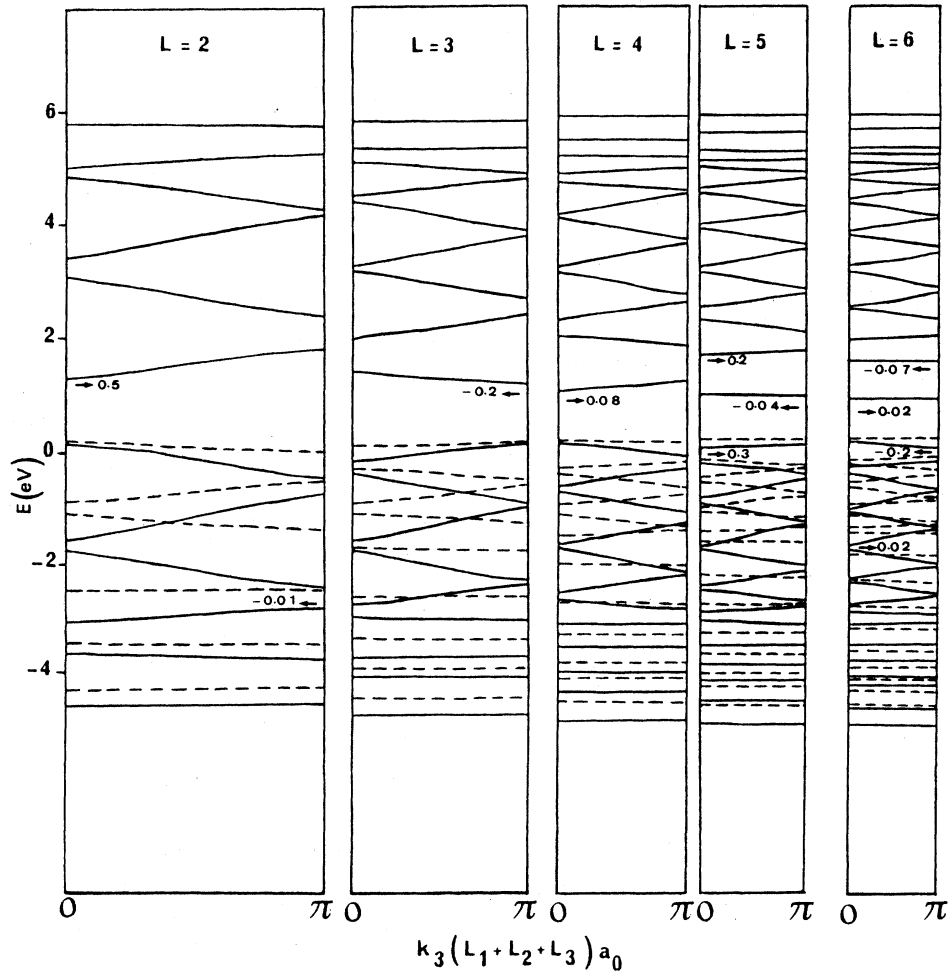


FIG. 4. Variation of electronic bulk and surface states of a triple-constituent GaSb/AlSb/InAs superlattice, terminated with an In plane (InAs surface layer) in function of k_3 for different layer thicknesses: $L_1=L_2=L_3=2$ to 6. The light-hole and electron bands are shown as solid lines and the heavy-hole bands as dashed lines. The position of some electronic surface states is indicated by arrows (\leftarrow or \rightarrow) together with the values of the corresponding decay factor $t(E_s)$.

The selected surface is labeled $(i\beta)$. For an N -layer superlattice, $2N$ surface configurations are possible, depending on the material terminating the semi-infinite superlattice. Each surface-material choice gives two configurations since the top plane may be composed of anions or cations for polar surfaces. For a given semi-infinite superlattice, the energy E_s of the surface states resolves the following equation:

$$D(E_s; i\beta; i'\beta') = 0. \tag{19}$$

As pointed out in Refs. 7 and 8, another condition is required in order to identify true surface states. Let us define the following quantities [where η is given by Eq. (10)]:

$$t = e^{\eta}, \tag{20}$$

$$t = \begin{cases} \eta - (\eta^2 - 1)^{1/2}, & \eta > 1 \\ \eta + i(1 - \eta^2)^{1/2}, & -1 < \eta < 1 \\ \eta + (\eta^2 - 1)^{1/2}, & \eta < -1 \end{cases}$$

and

$$A(E; i\beta; i'\beta') = -A_1 A_2 A_3 - \tilde{f}_i a_i d_i C_i C_i B_{i''} / \tilde{f}_i + \tilde{f}_{i''} a_i d_{i''} A_i C_i C_{i''} / \tilde{f}_i + \tilde{f}_i a_{i''} d_i A_i C_i C_{i''} / \tilde{f}_{i''}. \tag{21}$$

As $t(E_s)$ is the exponential decay factor associated with these surface states, the energy E_s of these states must fulfill the following condition:

$$|t(E_s)| < 1 \tag{22}$$

with

$$t(E_s) = A^{-1}(E_s). \tag{23}$$

The physical meaning of the condition (22) is that the electronic surface wave has to vanish exponentially as one moves off the surface towards the inner part of the superlattice.

We now have all the required elements to calculate the energies of possible surface states and to characterize their degree of localization. In what follows, we will con-

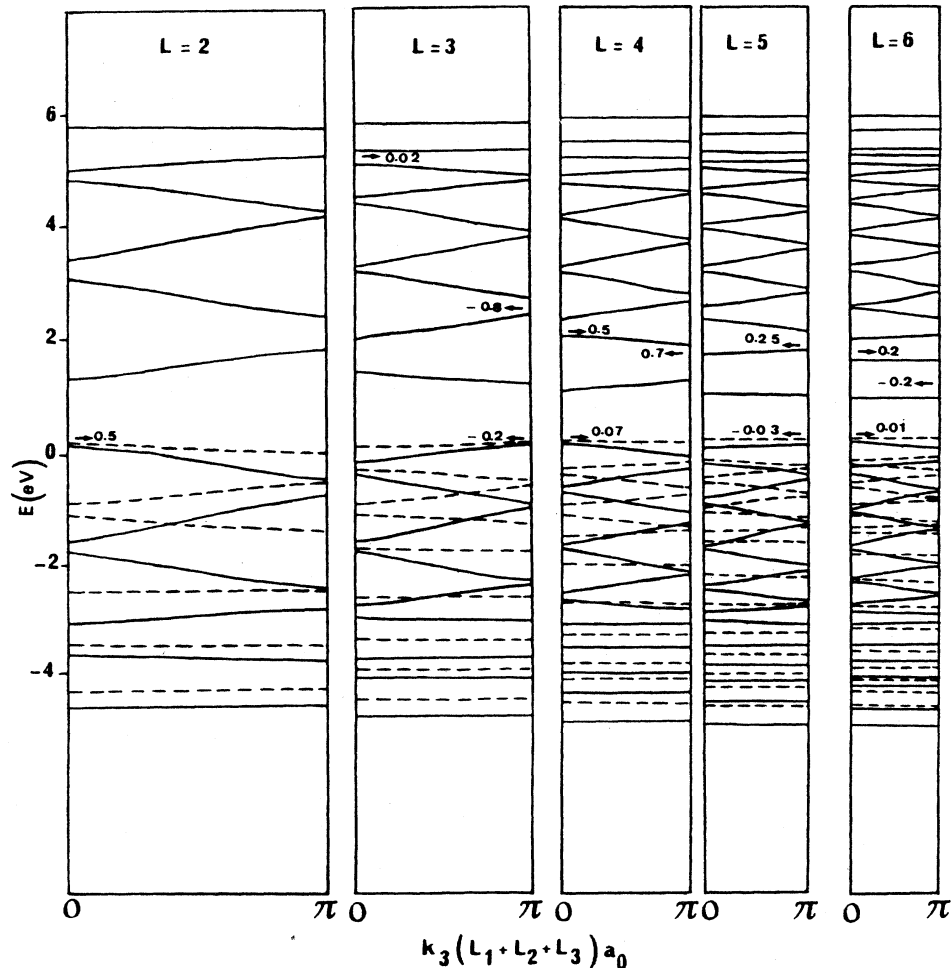


FIG. 5. Same as Fig. 4 for an anion (As)-terminated superlattice (InAs top layer).

sider the case of a three-constituent superlattice, namely the GaSb/AlSb/InAs heterostructure.

III. SURFACE ELECTRONIC STATES OF A THREE-CONSTITUENT SYSTEM

As explained before, six different surface configurations are possible. In order to calculate the energy of possible true surface states, we must solve the corresponding Eq. (19) for each configuration and check the validity of the condition (22). The required expressions of D are then obtained from Eq. (18) for the selected surface configuration ($i\beta; i'\beta'$).

In the surface calculation, we assume the transferability of all bulk interaction parameters to the surface layer because information on the way the surface may modify the bulk values is still lacking. A microscopic characterization of the structure of the surface layer will be necessary to obtain this information. The bulk parameters are those given in Ref. 11. Let us mention that the calculated surface states are indeed characteristic of the superlat-

tice. In our model, each separate constituent does not show surface states. We shall now discuss the results obtained. First of all, it is useful to compare the bulk superlattice electron dispersion relations with those of each bulk material constituting the superlattice. As we concentrate on possible surface states localized in the superlattice main gap, the comparison between the main gap associated with each separate material and that of the superlattice gives us an initial idea about the occurrence of such states as well as their origin. We describe the electronic bulk energy bands associated with GaSb, AlSb, InAs, and GaSb/AlSb/InAs superlattice bands in Fig. 1. These correspond to equal layer thickness $L_1=L_2=L_3=12$ and are represented as a function of the propagation-vector component perpendicular to the interface plane (k_3). The selected layer thicknesses ensure that the calculated bulk bands do indeed correspond to those of a very thick material. This enables us to discuss the calculated superlattice surface states in terms of the separate constituent bands. The latter have their energy split off because of extra interactions due to the superlat-

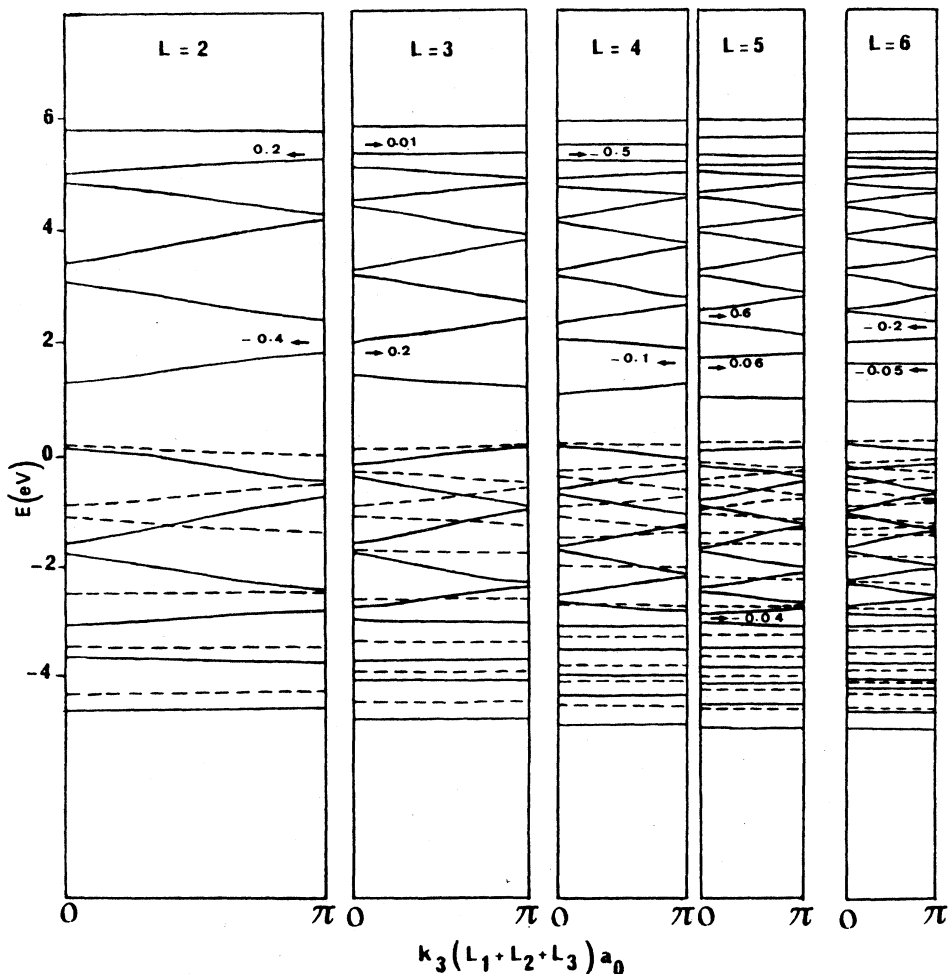


FIG. 6. Same as Fig. 4 for a cation (Ga)-terminated superlattice (GaSb top layer).

tice formation. Their folding arises because of the new periodicity of the heterostructure. One can notice the wide AlSb main gap in which InAs and GaSb gaps are embedded. The superlattice main gap is narrower than the constituent gaps because of the folding process. The top of the GaSb valence band is the closest to the top of the heavy- or light-hole superlattice bands, although situated higher in energy. The InAs and AlSb bands are situated below the corresponding superlattice bands. On the other hand, the bottom of the InAs conduction band is the closest to the analogous superlattice band. On the whole, this will ensure that the InAs main gap is the closest to the superlattice gap. Consequently, we anticipate that the InAs-terminated superlattice is the best candidate in supporting electronic surface states associated with anions or cations. In Fig. 2, we represent the calculated electron and light-hole bulk band energies and the bandwidth for the GaSb/AlSb/InAs superlattice as a function of

$$Q = 1 - \cos(k_1 a_0/2) \cos(k_2 a_0/2) \quad (24)$$

for layer thicknesses equal to $L_1 = L_2 = L_3 = 2$. In the same figure, we also give the dispersion relations associated with the main-gap surface states corresponding to a semi-infinite superlattice terminated with an InAs layer [curve 1 (2) corresponds to the cation (anion) top plane]. In order to estimate the degree of localization of these surface states, we calculate the exponential decay factor $t(E_s)$. Let us recall the meaning of this parameter. For small values of t , E_s is the energy of a true surface state, while values of t higher than 1 correspond to electron wave functions decaying slowly into the inner region of the superlattice. We observe quite a sensitive difference in the variations of t , according to whether they correspond to anion or cation states. For $Q=0$, the long-wavelength limit $t(E_s)$ is equal to 0.5 for both surface states. However, as we leave this limit, by increasing Q , the decay factor associated with anion-derived surface states (As) decreases more quickly than that associated with cation surface states (In). This feature is indeed well reproduced by the positions of the corresponding dispersion relations with respect to the bulk bands. While the

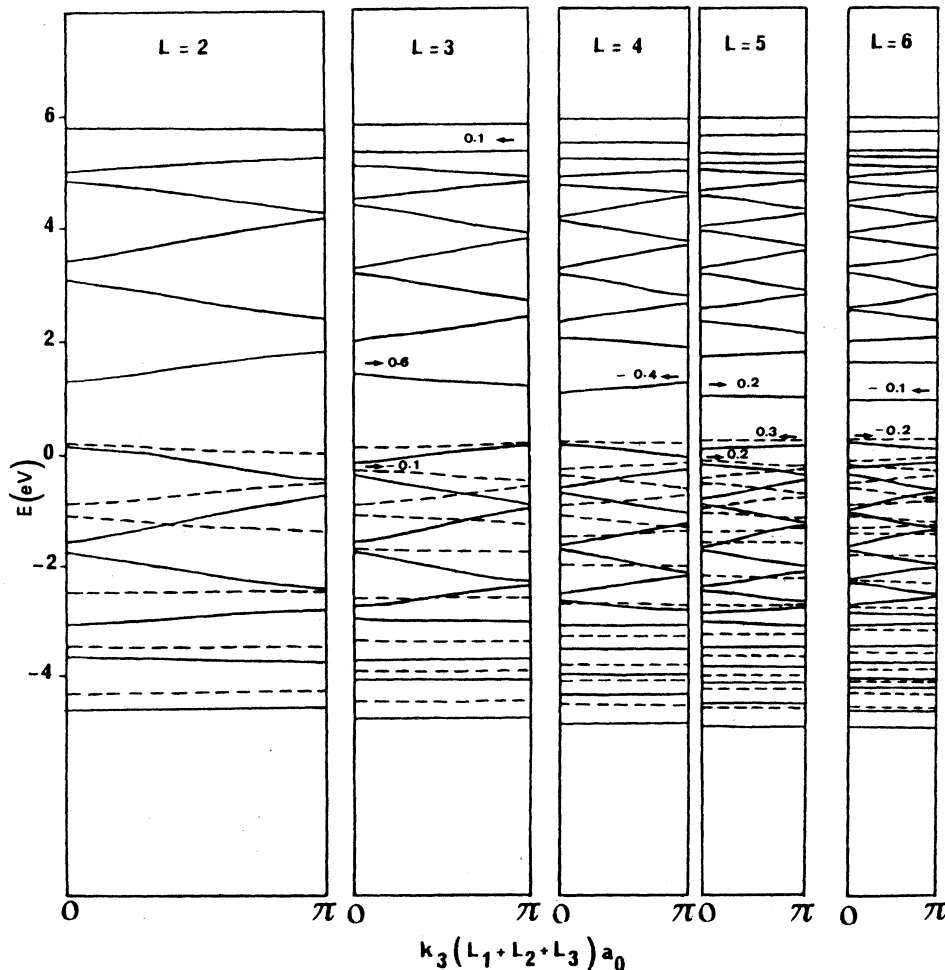


FIG. 7. Same as Fig. 4 for an anion (Sb)-terminated superlattice (GaSb top layer).

latter state is very close to the subband from which it originates, the former emerges as a level close to the middle of the superlattice main gap where t reaches values as small as 0.01.

Let us discuss the evolution of the energy of superlattice surface states with respect to layer thickness. Our interest in this problem is due to the possibility of discovering a new superlattice surface effect. Our study of the bulk electronic structure of the triple-constituent superlattice has shown that the E_1 and HH_1 (HH denotes heavy hole) levels are quite sensitive to the layer thickness L .¹¹ This effect is shown in Fig. 3 (dashed curves). We find that as L increases, these two levels become closer until an intersection occurs at a critical thickness. This will result in a semiconductor-semimetal transition. Because of their respective origins (cation surface states are derived from the conduction-band and anion surface states from valence bands), one may expect the occurrence of an analogous effect for these surface states. We represent in Fig. 3 the variation of the cation-derived surface state (curve 1) with respect to L . Our results show that level 1 does indeed follow the variation of level

E_1 . The effect is more pronounced for the cation-derived (In) level due to a strong interaction with the HH_1 level. As L increases, these two levels intersect for a thickness lower than that which corresponds to the bulk transition. This will result in an electron transfer to the cation-derived surface states. In the case of bulk transition, the level E_1 , to which the electrons are transferred, is a conduction level. However, we are now dealing with an electron transfer towards a surface-localized level. Although this level may partly acquire an electronic bulk characteristic by approaching the superlattice valence band, its surface localization may confine the transferred electrons. This may have important consequences for superlattice electronic surface features.

In Figs. 4-9, we show the position of some surface-state levels (indicated by \leftarrow or \rightarrow), associated with different superlattice surface configurations and localized in the superlattice gap. These are represented for increasing layer thicknesses. The numbers beside the arrows give the values of the corresponding decay factor t .

We next consider the GaSb-terminated superlattice. The cation-constituted surface configuration does not

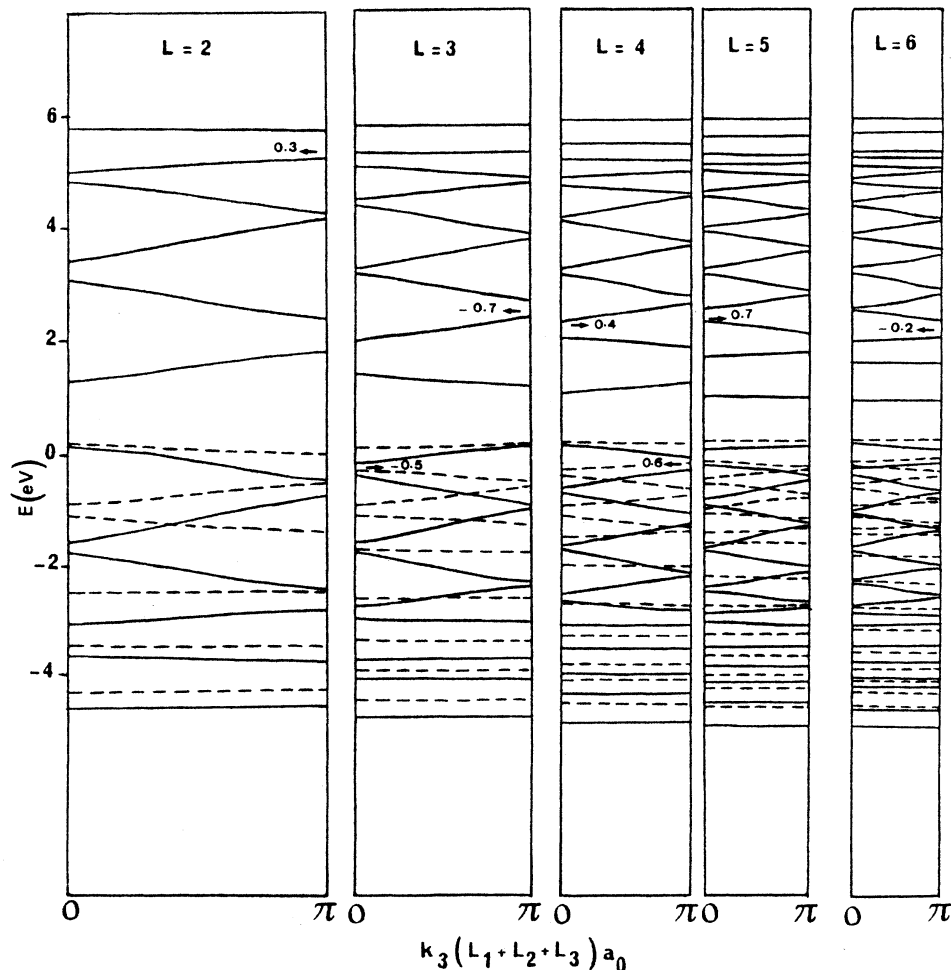


FIG. 8. Same as Fig. 4 for a cation (Al)-terminated superlattice (AlSb top layer).

show surface states localized within the main gap (Fig. 6). Anion-derived surface states exist for layer thicknesses where $L \geq 5$ (Fig. 7). In order to understand this result, one should bear in mind that the bottom of the GaSb bulk conduction band, from which the cation-derived state might arise, is very well separated from the superlattice main gap. Conversely, the top of the bulk valence band, from which the anion-derived surface state arises, falls inside that gap. Let us now compare the results for InAs (As top plane) and GaSb (Sb top plane) -terminated superlattices. As the top of the GaSb valence band is closer to the superlattice main gap (see Fig. 1), one may expect that an electronic surface state is, at least, equally probable for both configurations. However, our results show a strong dependence on layer thickness. For thin layers ($L < 5$), it is indeed the InAs-terminated superlattice which gives rise to anion (As) -derived surface states whose energy is localized in the superlattice main gap. Anion (Sb) -derived surface states appear for $L \geq 5$. In order to understand this result, one may also invoke the presence of Sb atoms in the AlSb layer below the GaSb

surface layer. For thin GaSb layers, a strong interaction exists between Sb atoms, situated in the GaSb and AlSb layers. If we consider that the top of the AlSb valence band is situated well below that of GaSb, we must refer to a mixed (between AlSb and GaSb) valence level lower than that of GaSb. This may explain the absence of such Sb surface states for thin layers where the superlattice regime predominates. As the thickness of the GaSb layer increases, the intrinsic electronic features of GaSb predominate because of the weakness of direct Sb (in GaSb)-Sb (in AlSb) interactions. The valence level, from which the Sb-derived surface states emerge for $L \geq 5$, is now closer to the GaSb valence level. This layer-thickness effect reflects the competition between two regimes in which multiple- or single-layer features dominate in obtaining superlattice surface states.

Eventually, the AlSb-terminated superlattice does not show surface-state features in the main gap for the selected layer thicknesses. This is due to the bulk band edges which are situated very far from the superlattice main gap (Figs. 8 and 9).

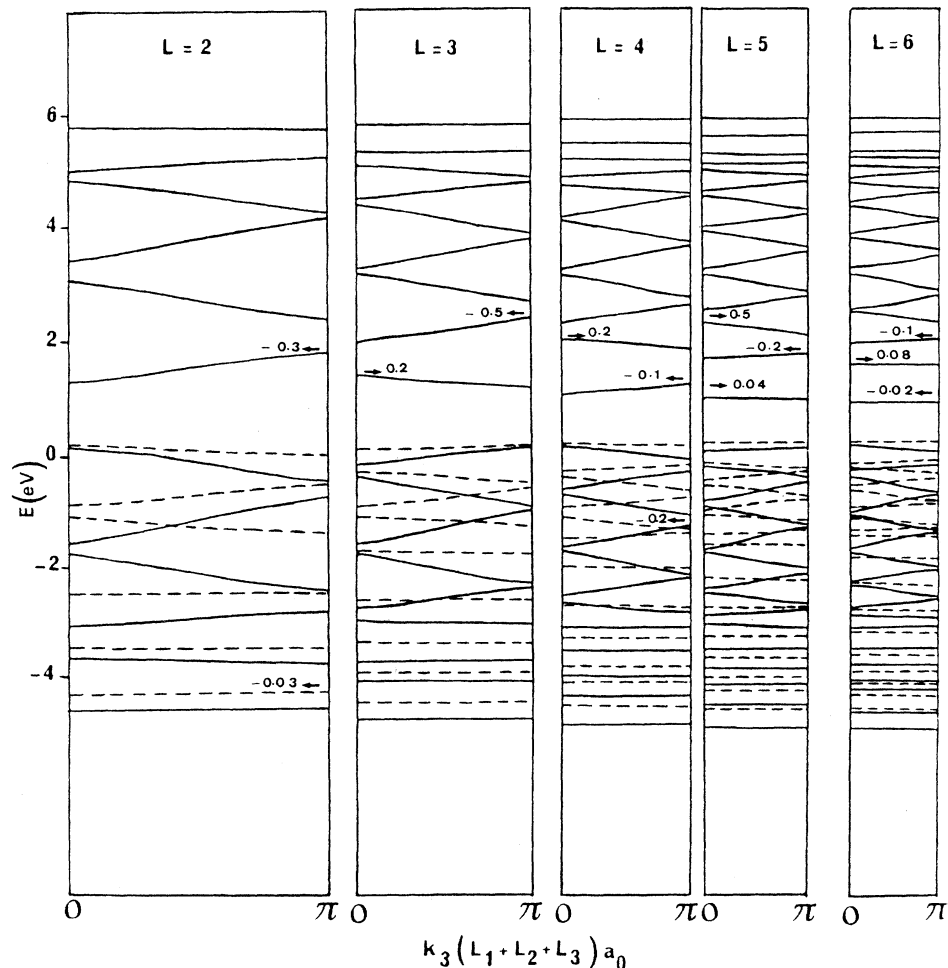


FIG. 9. Same as Fig. 4 for an anion (Sb) -terminated superlattice (AlSb top layer).

IV. CONCLUSION

In this work, we give the first calculation for surface-electronic states associated with a triple-constituent semiconductor superlattice. A simple two-band model is used to describe the bulk electron bands of each material and of the heterostructure. Analytic expressions of the surface response function of an N -layer superlattice are then obtained. These enable us to calculate the energy of possible surface states as well as the decay factor of the corresponding electronic wave function.

An application is made in the case of a triple-constituent superlattice, namely GaSb/AlSb/InAs. Six different surface configurations are then considered. For each of these configurations, we calculate the energy of surface states close to the superlattice main gap and we study their evolution in function of the layer thickness. In the case of a superlattice terminated with an InAs lay-

er and an In top plane, we have discovered the occurrence of a new electronic surface transition. This transition takes place when the cation (In) -derived surface-state level intersects the HH_1 level for a critical thickness lower than that for the bulk transition. This may result in new superlattice electronic surface properties. We believe that our result is not model dependent as the same simple model has given evidence for the bulk HH_1-E_1 transition in the case of the GaSb/InAs superlattice. We hope that this study will stimulate further investigations on surface and interface properties of this very interesting heterostructure.

ACKNOWLEDGMENTS

The Laboratoire d'Etudes des Surfaces, Interfaces et Composants, "Unité associée au Centre National de la Recherche Scientifique No. D 07870."

¹L. Esaki, IEEE J. Quantum Electron. **QE-22**, 1611 (1986), and references therein.

²J. R. Hayes and A. F. J. Levi, IEEE J. Quantum Electron. **QE-22**, 1744 (1986).

³T. H. Chiu and A. F. J. Levi, J. Vac. Sci. Technol. B **6**, 674 (1988).

⁴G. A. Sai-Halasz, R. Tsu, and L. Esaki, Appl. Phys. Lett. **30**, 651 (1977).

⁵L. Esaki, L. L. Chang, and E. E. Mendez, Jpn. J. Appl. Phys. **20**, L529 (1981).

⁶L. Dobrzynski, Surf. Sci. Rep. **6**, 118 (1986).

⁷P. Masri and L. Dobrzynski, Surf. Sci. **198**, 285 (1988).

⁸P. Masri, L. Dobrzynski, B. Djafari-Rouhani, and J. O. A. Idioudi, Surf. Sci. **166**, 301 (1986).

⁹G. A. Sai-Halasz, L. Esaki, and W. A. Harrison, Phys. Rev. B **18**, 2812 (1978).

¹⁰W. Ho, S. L. Cunningham, W. H. Weinberg, and L. Dobrzynski, Phys. Rev. B **12**, 3027 (1975).

¹¹M. D. Rahmani, P. Masri, and L. Dobrzynski, J. Phys. C **21**, 4761 (1988).